This article has been accepted for inclusion in a future issue of this journal. Content is final as presented, with the exception of pagination.

Analysis of Data Acquisition Time on Soil Moisture Retrieval From Multiangle L-Band Observations

Sandy Peischl, *Member, IEEE*, Jeffrey P. Walker, *Senior Member, IEEE*, Dongryeol Ryu, *Member, IEEE,* and Yann H. Kerr, *Senior Member, IEEE*

***Abstract*— This paper investigated the sensitivity of passive microwave L-band soil moisture (SM) retrieval from multiangle airborne brightness temperature data obtained under morning and afternoon conditions from the National Airborne Field Experiment conducted in southeast Australia in 2006. Ground measurements at a dryland focus farm including soil texture, soil temperature, and vegetation water content were used as ancillary data to drive the retrieval model. The derived SM was then in turn evaluated with the ground-measured near-surface SM patterns. The results of this paper show that the Soil Moisture and Ocean Salinity target accuracy of 0.04 $m^3 \cdot m^{-3}$ for single-SM retrievals is achievable irrespective of the 6 A.M. and 6 P.M. overpass acquisition times for moisture conditions $\leq$0.15 $m^3 \cdot m^{-3}$. Additional tests on the use of the air temperature as proxy for the vegetation temperature also showed no preference for the acquisition time. The performance of multiparameter retrievals of SM and an additional parameter proved to be satisfactory for SM modeling—independent of the acquisition time—with root–mean-square errors less than 0.06 $m^3 \cdot m^{-3}$ for the focus farm.**

***Index Terms*— Acquisition time, L-band, multi-incidence angle, passive microwave remote sensing, soil moisture (SM), soil moisture and ocean salinity (SMOS).**

I. Introduction

ONE of the main motivations for earth observing satellite missions is the enhancement of meteorological and climatic model predictions. Among others, the global soil moisture (SM) is considered as a significant input parameter to enhance model forecasts of climate and weather evolution. After decades of intensive research in near-surface SM remote sensing, the application of passive microwave observations has been proved to be most promising [1]–[4].

Manuscript received March 13, 2017; revised July 18, 2017 and August 27, 2017; accepted August 27, 2017. This work was supported by the Australian Research Council (ARC) through Infrastructure Grant LE0453434 and Grant LE0560930 and Research Grant DP0557543. The initial setup and maintenance of the Murrumbidgee catchment monitoring system was funded by the CRC for Catchment Hydrology and the ARC under Grant DP0343778 and Grant DP0557543. *(Corresponding author: Sandy Peischl.)*

S. Peischl and J. P. Walker are with the Department of Civil Engineering, Faculty of Engineering, Monash University, Melbourne, VIC 3800, Australia (e-mail: sandy.peischl@gmail.com; jeff.walker@monash.edu).

D. Ryu is with the Department of Infrastructure Engineering, Melbourne School of Engineering, University of Melbourne, Melbourne, VIC 3010, Australia (e-mail: dryu@unimelb.edu.au).

Y. H. Kerr is with the Centre d'Etudes Spatiales de la Biosphère, 31401 Toulouse, France (e-mail: yann.kerr@cesbio.cnes.fr).

Color versions of one or more of the figures in this paper are available online at http://ieeexplore.ieee.org.

Digital Object Identifier 10.1109/TGRS.2017.2757025

Not only has the L-band (1.4 GHz) passive microwave satellite launched in 2009 by the European Space Agency heralded the first dedicated mission for global soil moisture and ocean salinity (SMOS) mapping [5], [6], but also its novel design provides a unique opportunity to utilize multiangle observations of the same area on the ground to derive the ancillary information required in the SM retrieval more reliably. Moreover, the SMOS mission has a two- to three-day revisit cycle, designed around a polar sun-synchronous orbit with a 6 A.M. local solar time ascending node and 6 P.M. descending node, the emphasis being on the 6 A.M. overpass time for SM retrieval [7].

The basis for SM measurement from SMOS is the relationship between a measured brightness temperature (TB) and the dielectric constant of the near-surface soil, which is in turn related to its moisture content. With this SM relationship being affected by a range of factors, including surface roughness and vegetation cover (e.g., type, vegetation water content (VWC), growth state, and litter presence), the SMOS mission uses the multi-incidence angle observations to derive some of the ancillary parameters (e.g., vegetation optical depth and surface roughness) and hence facilitate the retrieval algorithm. However, the emphasis to date has been on the morning SMOS overpass, as the ideal conditions for SM retrieval at L-band are generally assumed to be around dawn when the Faraday rotation occurring in the ionosphere is at its minimum [8], [9] and the top soil column is in close thermal equilibrium with the overlying canopy. The latter simplifies the model by assuming an effective temperature that represents both the near-surface soil and canopy temperature, implying that there is no temperature gradient in the vegetation or soil profile. However, the afternoon SMOS observations might also hold valuable SM information, and indeed yield better SM retrievals in places like Europe where the ascending SMOS data are often corrupted due to radio frequency interference (RFI) [10], [11], requiring filtering or in severe case even complete masking. These findings were supported by the study presented by Al-Yaari *et al.* [12], who compared the SMOS L3 SM products from ascending and descending overpasses with reference surface SM products derived from the AMSR-E satellite and a land data assimilation product provided by the European Centre for Medium Range Weather Forecasts. Further varying patterns in the accuracy of retrieval products obtained from active and passive microwave satellite sensors at different acquisition times were also demonstrated by Lei *et al.* [13].

II. Radiative Transfer Model

The model used for simulating the grass canopy emission at L-band in this paper is one of the core algorithms applied to SMOS data [7]. A detailed description of the L-band Microwave Emission for the Biosphere (L-MEB) model can be found in [14], so only the pertinent details are given here. In brief, inversion of the model allows the retrieval of near-surface SM and additional model parameters by minimizing the root-mean-square error (RMSE) between observed and simulated TBs using initial ancillary input and SM assumptions.

In L-MEB, the individual contributions of the soil and vegetation media and their interaction on the composite TB are accounted for using a radiative transfer approach called the tau–omega model [15], [16]

$$\begin{aligned}\mathrm{TB}(P,\theta) = (1-\omega(P)) \times (1-\gamma(P,\theta)) \times (1+\gamma(P,\theta)\\ \times \mathrm{rG}(P,\theta)) \times \mathrm{TC} + (1-\mathrm{rG}(P,\theta))\\ \times \gamma(P,\theta) \times \mathrm{TG} \quad (1)\end{aligned}$$

with P representing the polarization (H: horizontal and V: vertical), θ representing the incidence angle, and TG and TC corresponding to the effective soil and vegetation temperature [K], respectively. The reflectivity of nonsmooth soil surfaces rGP, which is sensitive to the incidence angle and polarization, can be quantified using a modification of the Fresnel equation by including soil roughness parameters HR and NR(P)

$$G(P,\theta) = r \times G(P,\theta) \times \exp[-\mathrm{HR} \times \cos\theta(\mathrm{NR}(P))]. \quad (2)$$

The Fresnel reflectivity from a smooth, ideally flat surface $r \times G(P, \theta)$ can in turn be related to SM content through a dielectric mixing model such as that developed by Dobson *et al.* [17] or Mironov *et al.* [18]. The latter is used in this paper. The model variables characterizing the canopy are single scattering albedo $\omega(P)$ and vegetation transmissivity $\gamma(P)$; the latter, also known as vegetation attenuation, is modeled as a function of the incidence angle and the optical depth at nadir $\tau\mathrm{NAD}$

$$\gamma(P,\theta) = \exp[-\tau\mathrm{NAD} \times (\sin 2\theta \times \mathrm{tt}(P)) + (\cos 2\theta)/\cos\theta] \quad (3)$$

with the vegetation structure parameters tt(P) correcting the optical depth for nonnadir views at each polarization. Hence, the optical depth increases with the amount of water on/in the canopy, which consequently reduces the transmission of the emitted soil energy within the vegetation medium. L-MEB uses the commonly assumed linear relationship between the VWC and the nadir optical depth

$$\tau\mathrm{NAD} = \mathrm{VWC} \times b(P) \quad (4)$$

where the empirical vegetation parameter $b(P)$ is mainly dependent on the sensor frequency, polarization, canopy type, and plant structure [19].

III. Experimental Data Set

This paper is based on airborne measured L-band TBs acquired during the National Airborne Field Experiment (NAFE) in Australia, which is described extensively in [20]. The NAFE campaign was conducted for a three-week period in November 2006 in the central region of the Murrumbidgee River catchment, NSW, Australia. The primary instrument aboard the aircraft was the Polarimetric L-band Multibeam Radiometer (PLMR), which operates at a frequency of 1.413 GHz with a 24-MHz bandwidth. Dual-polarized measurements are acquired through polarization switching, with an accuracy of 3 and 2 K for V- and H-polarizations, respectively [21]. The PLMR is a patch-array antenna capable of scanning the surface depending on pitch of the aircraft with three viewing angles (±7°, ±21.5°, and ±38.5°) in forward and backward directions of the flight axis, when used in along-track configuration.

The NAFE'06 multiangle flights were undertaken along a 75-km-long transect line in the Yanco region of the Murrumbidgee River catchment, with a triple repetition per flight and spatial resolution of about 500 m (Fig. 1). For comparison with SMOS characteristics, the prelaunch of SMOS flights was centered around both 6 A.M. and 6 P.M. local solar times, coinciding with the ascending and descending SMOS overpasses. A total of six flight days with three morning and three afternoon flights were available for this study, which is the first to utilize this multiangle aspect of the NAFE'06 data set [20].

The airborne observations were supported by ground measurements at three focus areas located along the flight transect. These so-called focus farms were of approximately 1 km × 3 km in size, and chosen to be colocated with the permanent OzNet monitoring stations [22]. The long-term OzNet stations mainly provide time series of profile SM, profile soil temperature, and rainfall observations. In addition, monitoring at the focus farms was supplemented with temporary NAFE stations, which provided profile SM and soil temperature, as well as rainfall and thermal infrared (TIR) data of either the soil surface in the case of bare soil or the canopy layer in the case of vegetation cover. Supplementary data were collected by assigned ground teams focusing on the following:

1) near-surface SM measurements using the Hydraprobe Data Acquisition System (HDAS) [23];
2) biomass characterization including VWC, surface reflectance, and leaf area index (LAI);
3) surface roughness measurements across each individual farm using a pin profiler.

The three focus farms that were covered by the transect flight included two dry land farms (Y7, Y10) with pasture as dominant land use and one irrigated farm (Y1) with different types of crops such as wheat, barley, and maize. This paper focused on data collected across farm Y7 (see Fig. 1), which demonstrated a natural variability in SM from 0.03 to 0.12 $\mathrm{m^3{\cdot}m^{-3}}$ in response to a few small rainfall events throughout the campaign. Biomass samples obtained across the dry land focus farms demonstrated rather low VWC of ~0.08 $\mathrm{kg{\cdot}m^{-2}}$, whereas for vegetation samples obtained at

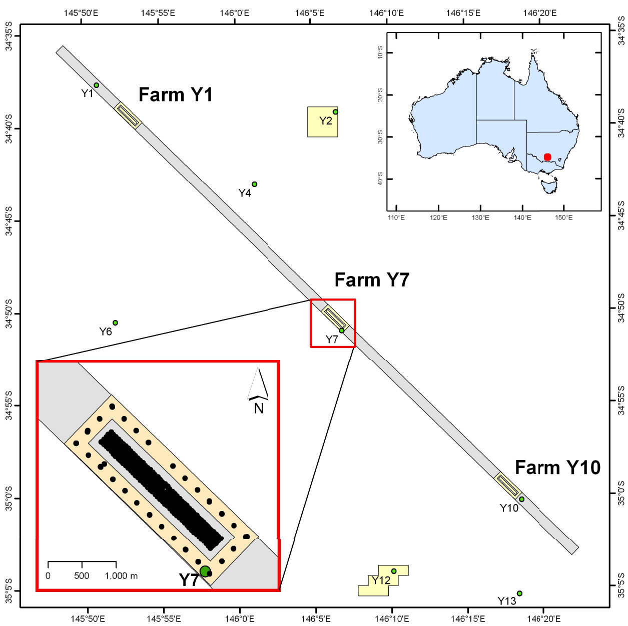

Fig. 1. (Top) Location of the NAFE'06 focus farms Y1, Y7, and Y10 and the OzNet monitoring network (green dots) within the Yanco study area. (Bottom inset) Y7 focus farm which was covered by multiangle transect flights (gray shade), location of the corresponding monitoring station Y7, and distribution of the intensive SM sampling grid (black points).

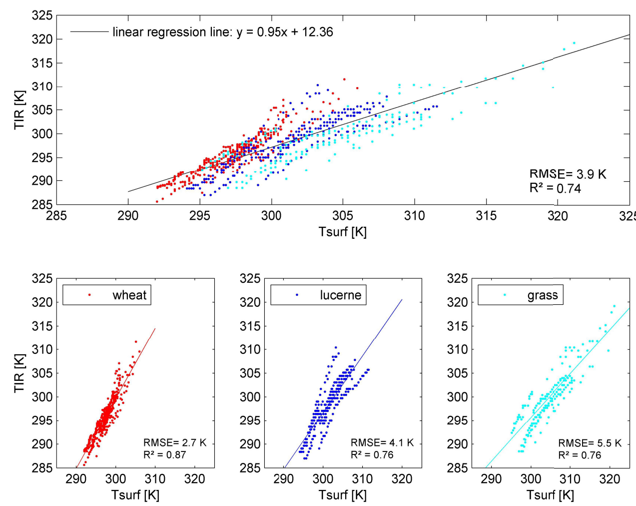

Fig. 2. Linear regression applied to ground-measured TIR and surface soil temperature (T_{surf}) from 1-cm-depth measurements considering three types of vegetation cover.

TABLE I
DAILY VARIABLE L-MEB INPUT PARAMETERS FOR FARM Y7

Date [DD/MM/YYYY]	SM (std) [m^{3}m^{-3}]	VWC [kg m^{-2}]	Tsurf [K]	Tdeep [K]
01/11/2006	0.02 (0.02)	0.03	293	297
03/11/2006	0.12 (0.02)	0.17	306	297
08/11/2006	0.05 (0.02)	0.03	292	296
10/11/2006	0.04 (0.02)	0.03	309	303
15/11/2006	0.13 (0.04)	0.17	288	295
17/11/2006	0.10 (0.03)	0.10	304	300

the irrigated cropping site Y1, VWC of 0.3–1.8 kg·m^{-2} was measured (Table I).

IV. MULTIANGLE SOIL MOISTURE RETRIEVAL

The multiangle retrieval was performed using the L-MEB retrieval algorithm developed for processing SMOS data [24]. The parameterization of soil texture, soil profile temperature, and bulk density was based on the available ground measurements taken at or nearby focus farm Y7 (Table II). Supplementary information for the characterization of grass cover and surface roughness in the model was sourced from [25] and [26]. Table II presents the main model parameterization applied to all observation days. The design of the focus farm and the spatial resolution of PLMR yielded a total of five independent PLMR pixels colocated at the farm with a size of approximately 500 m × 500 m each. Within each of these pixels, all angular TB measurements from the triple flight repetitions were gathered and applied to L-MEB so as to facilitate the multiangle SM retrieval per pixel. A total of four retrieval scenarios for each of the morning and afternoon data sets were studied, which are as follows:

1) 1P single-parameter retrieval of SM;
2) 2P retrieval of SM and VWC;
3) 2P retrieval of SM and surface roughness (SM–HR);
4) 2P retrieval of SM and vegetation temperature.

Regarding the afternoon retrieval, two different approaches with respect to the vegetation temperature information, which is essential to run the L-MEB model, were tested. First, the vegetation temperature was set equal to the air temperature, as per the morning overpasses, where it is commonly assumed that the vegetation temperature is expected to be close to the air temperature at dawn. Second, the afternoon vegetation temperature was estimated from a linear regression derived between surface soil temperature T_{surf} at 1-cm-depth and TIR temperature measurements of the overlying canopy (see Fig. 2). The relationship was determined for specific types of vegetation as well as for a mixed vegetation cover. Note that only the duration of the afternoon overpass between 4:30 and 7:00 P.M. local solar times was considered when establishing the relationship. Both options, either using T_{air} or using the TIR–T_{surf}-derived vegetation temperature, were tested as input to run the L-MEB model. Even though the difference between the observed temperature T_{air} and the TIR–T_{surf}-derived vegetation temperature for the afternoon overpass was up to 12 K for different dates, the forward modeling yielded no significant improvement (<0.03 K) when the TB predictions were compared with the observed TB responses across various dates and angular ranges measured. The authors would like to point out that the SM and vegetation conditions captured during the field campaign showed limited range across the test dates, so the impact of higher moisture conditions with respect to the afternoon vegetation temperature and the subsequent effect on the SM retrieval algorithm could not be fully tested with this data set. The AACES field campaigns, which covered the whole Murrumbidgee catchment including the NAFE'06 test sites, will offer a wider range of SM conditions for further analysis [27].

TABLE II

FIXED L-MEB INPUT PARAMETERS FOR FARM Y7

Soil texture [%]		Bulk density	Roughness [-]			Vegetation [-]			
Sand	Clay	[g m^{-3}]	HR	Q	NR(P)	b	ω(V)	ω(H)	tt(P)
39	25	1.3	0.5	0	0	0.15	0.05	0	1

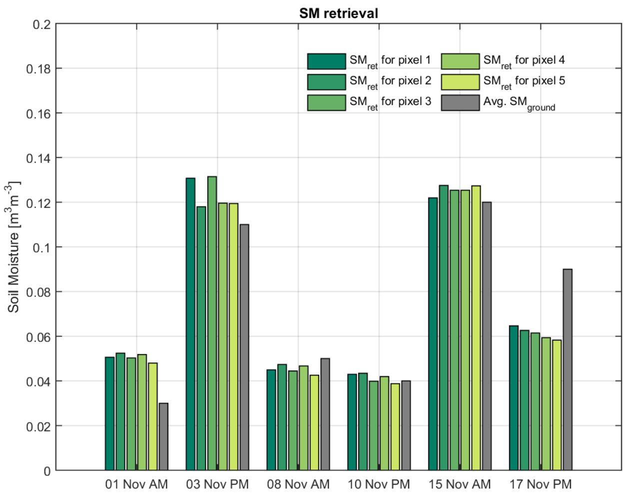

Fig. 3. Comparison of 1P-retrieved soil moisture values (SMret) across the focus farm Y7 per PLMR pixel (green shades) with the farm-averaged ground-measured HDAS (average SMground in gray shades) observations per sampling day. AM: morning flight. PM: afternoon flight.

TABLE III

RMSE OF THE RETRIEVAL RESULTS FOR SM COMPARED WITH MEASUREMENTS AT FARM Y7

Date [DD/MM/YYYY]	1P retrieval SM [m^{3}m^{-3}]	2P retrieval SM-HR [m^{3}m^{-3}]	SM-VWC [m^{3}m^{-3}]	SM-Tveg [m^{3}m^{-3}]
01/11/2006	0.02	0.04	0.02	0.02
03/11/2006	0.02	0.02	0.01	0.02
08/11/2006	0.01	0.01	0.00	0.00
10/11/2006	0.00	0.05	0.01	0.00
15/11/2006	0.01	0.06	0.00	0.00
17/11/2006	0.03	0.02	0.02	0.03
RMSE max	0.03	0.06	0.02	0.03
RMSE average	0.01	0.03	0.01	0.01

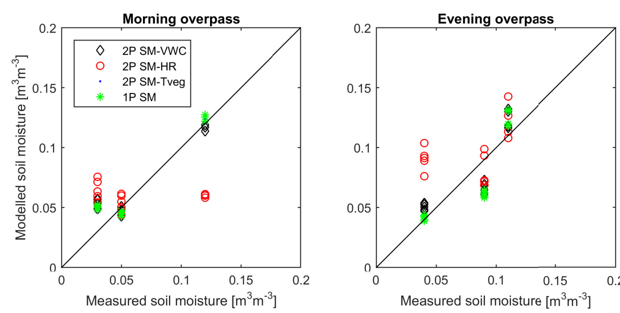

Retrieval scenario	RMSE AM [m^{3}m^{-3}]	RMSE PM [m^{3}m^{-3}]
1P SM	0.01	0.02
2P SM-VWC	0.01	0.02
2P SM-HR	0.04	0.03
2P SM-Tveg	0.01	0.02

Fig. 4. Comparison of retrieved soil moisture values across the focus farm Y7 per PLMR pixel with the ground-measured HDAS information classified into morning (6 A.M.) and afternoon (6 P.M.) observations.

A. Spatial Soil Moisture Pattern at Farm Scale

The single-parameter retrieval of SM conditions for all five PLMR pixels at focus farm Y7 are compared with the ground-measured near-surface SM content in Fig. 3. Across the five pixels, and hence within the entire focus farm, there were only minor variations in SM observed per day with the standard deviation of HDAS measurements ranging between 0.02 and 0.04 m^3·m^{-3}. Similar variations were achieved across the five PLMR pixels from L-MEB retrievals. Direct comparison with the averaged ground-measured SM per farm and observation day demonstrated a good agreement with the model predictions with RMSE values of $\leq$0.03 m^3·m^{-3}. The model results captured the variabilities and the magnitudes of SM across the test dates caused by two precedent rain events, on November 2 with 5-mm rainfall and on November 13 with 10.4-mmrainfall.

By introducing a second unknown parameter and running a 2P retrieval model, the modeled SM yielded similar RMSE values of less than 0.03 m^3·m^{-3} when SM was derived simultaneously with either VWC or vegetation temperature (Table III). In the case of the SM–HR retrieval scenario, the corresponding RMSE was on average 0.03 m^3·m^{-3} with a peak of 0.06 m^3·m^{-3} for one test date.

B. Comparison of Acquisition Time

In order to study the effect of acquisition time on the SM retrieval performance using TB data acquired at various incidence angles, the model results for all retrieval scenarios (single- and multiparameter retrievals) were classified into morning and afternoon. Consequently, the model-retrieved SM values were compared with the ground-measured near-surface SM conditions across the field campaign and quantified in terms of the RMSE (see Fig. 4).

Across the range of moisture conditions captured during the NAFE’06 campaign, only minor variations were observed between the model predictions and the *in situ* measurements. In general, the difference was between 0.01 and 0.04 m^3·m^{-3} for morning overpasses and 0.02 and 0.03 m^3·m^{-3} for evening overpasses—all results being well within the desired SMOS target accuracy. Comparison of the three morning and three afternoon flights did not exhibit any significant difference or preference in acquisition time for SM retrieval modeling. Thus, providing rather low SM conditions, no degradation of SM quality is expected when using the descending overpass L-band data from SMOS. Moreover, there may even

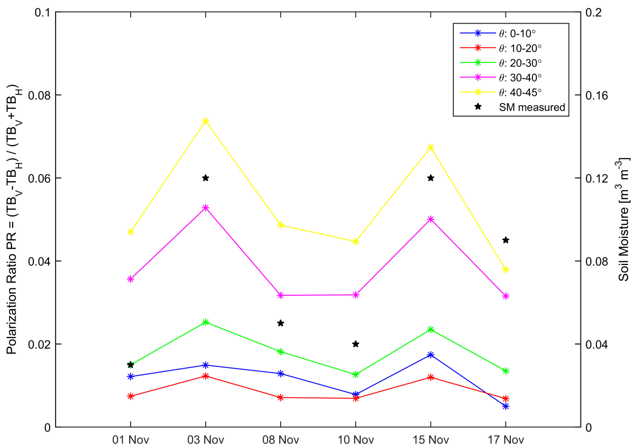

Fig. 5. Comparison of PRs between the vertical and horizontal TB observations measured during the course of the NAFE'06 field campaign. Overlain is the HDAS SM information averaged from all samples taken across focus farm Y7.

be an improved accuracy in places like Europe where descending SMOS data are less affected by RFI than are ascending data [8], [9].

V. Polarization Index Analysis

Further analysis of the NAFE'06 data set focused on calculation of the polarization ratio (PR) (difference between the horizontal and the vertical brightness observations divided by the sum). The index is a normalized quantity which describes the decreasing deviation from horizontal and vertical emissivities corresponding to the increase of LAI. Since the contribution of the vegetation layer to the emission is unpolarized and tends to be rather independent of the polarization, the PR is often used to gather information on the vegetation canopy, its density, and evolution. Moreover, the index demonstrates a strong dependence on SM content and varies from approximately 0.04 to 0.22 within the range of SM encountered.

The NAFE' 06 TB data were classified into five assigned angular groups and the individual PR per incidence angle determined for each sampling day (Fig. 5). Generally, there was a higher PR for incidence angles $>30°$ than that for the smaller incidence angles, resulting in two groups of PRs for all six sampling days tested. As described in [28] for view angles $>30°$, there is a distinct difference in PR for bare soils due to TBH being significantly larger than TBV. With increasing vegetation presence, the signal becomes progressively depolarized, ultimately resulting in TBH $\approx$ TBV for dense vegetation. Consequently, with regard to the previous analysis of the air temperature T_{air} versus the TIR–T_{surf}-derived vegetation temperature as a proxy for model parameterization in terms of the canopy and surface temperature in the afternoon, the demonstrated PR behavior supports the earlier findings. The noticeable contrast between the low and high angular groups and the related PR implies a rather sparse vegetation cover which in turn allows a strong emission from the soil without major scattering effects due to overlaying vegetation. Thus, the usage of the TIR–T_{surf}-derived vegetation temperature might not be able to demonstrate its full potential for the given surface conditions.

Visual inspection of all PRs against the observed SM certainly presented a trend with respect to the moisture conditions across all angular groups tested. There was an overall increase in the PR with an increase in SM, as expected due to the higher polarization impacts on the soil emission with higher water content. Moreover, the slope varied across the groups, being higher for the large angular observations compared to the small angular measurements.

VI. Conclusion

This paper studied the SM retrieval performance from airborne L-band observations in Australia for different times of data acquisition. The multiangle radiometer data were available for three morning flights around 6 A.M. local solar time and three afternoon flights around 6 P.M. local solar time, closely matching the ascending and descending overpass times of SMOS. For SM retrieval over this pastured study site, the L-MEB model was parameterized using ground measurements in combination with empirical variables sourced from the literature. The results showed that providing a sparse dryland vegetation cover and rather low SM conditions for afternoon retrievals, the canopy and surface soil temperature information might be used as for early morning measurements, by assuming air temperature values for both. It was not possible to check the effect of higher SM and dense vegetation presence on this assumption.

The comparison of the SM retrieval performance under morning and afternoon acquisition times yielded similar results, with all being less than or equal to the SMOS target accuracy of 0.04 $m^3 \cdot m^{-3}$ for the SMOS L2 SM product. These findings were consistent throughout the numerous retrieval scenarios that were tested in this paper, including single- as well as multiparameter retrievals.

Acknowledgment

The authors would like to thank the National Airborne Field Experiment 2006 Team for collecting and providing the data set used in this paper.

References

[1] T. J. Jackson, "III. Measuring surface soil moisture using passive microwave remote sensing," *Hydrol. Process.*, vol. 7, no. 2, pp. 139–152, 1993.

[2] E. G. Njoku and D. Entekhabi, "Passive microwave remote sensing of soil moisture," *J. Hydrol.*, vol. 184, pp. 101–129, Oct. 1996.

[3] J. P. Walker and P. R. Houser, "Requirements of a global near-surface soil moisture satellite mission: Accuracy, repeat time, and spatial resolution," *Adv. Water Resour.*, vol. 27, no. 8, pp. 785–801, Aug. 2004.

[4] T. Schmugge, P. E. O'Neill, and J. R. Wang, "Passive microwave soil moisture research," *IEEE Trans. Geosci. Remote Sens.*, vol. GRS-24, no. 1, pp. 12–22, Jan. 1986.

[5] Y. H. Kerr *et al.*, "The SMOS mission: New tool for monitoring key elements of the global water cycle," *Proc. IEEE*, vol. 98, no. 5, pp. 666–687, May 2010.

[6] Y. H. Kerr, P. Waldteufel, J. P. Wigneron, J. Martinuzzi, J. Font, and M. Berger, "Soil moisture retrieval from space: The Soil Moisture and Ocean Salinity (SMOS) mission," *IEEE Trans. Geosci. Remote Sens.*, vol. 39, no. 8, pp. 1729–1735, Aug. 2001.

[7] Y. H. Kerr, P. Waldteufel, P. Richaume, J.-P. Wigneron, P. Ferrazzoli, and R. J. Gurney, "SMOS level 2 processor for soil moisture—Algorithm theoretical based document (ATBD)," CESBIO, Toulouse, France, Tech. Rep. SO-TN-ESL-SM-GS-0001, Jan. 2011.
[8] S. H. Yueh, "Estimates of Faraday rotation with passive microwave polarimetry for microwave remote sensing of Earth surfaces," *IEEE Trans. Geosci. Remote Sens.*, vol. 38, no. 5, pp. 2434–2438, Sep. 2000.
[9] *Ionospheric Propagation Data and Prediction Methods Required for the Design of Satellite Services and Systems*, document Rec. ITU-R P.531-6, Geneva, Switzerland, 2001.
[10] A. Camps, J. Gourrion, J. M. Tarongí, A. Gutierréz, J. Barbosa, and R. Castro, "RFI analysis in SMOS imagery," in *Proc. IEEE Int. Geosci. Remote Sens. Symp. (IGARSS)*, Honolulu, HI, USA, Jul. 2010, pp. 2007–2010.
[11] R. Oliva *et al.*, "SMOS radio frequency interference scenario: Status and actions taken to improve the RFI environment in the 1400–1427-MHz passive band," *IEEE Trans. Geosci. Remote Sens.*, vol. 50, no. 5, pp. 1427–1439, May 2012.
[12] A. Al-Yaari *et al.*, "Global-scale evaluation of two satellite-based passive microwave soil moisture datasets (SMOS and AMSR-E) with respect to Land Data Assimilation System estimates," *Remote Sens. Environ.*, vol. 149, pp. 181–195, Jun. 2014.
[13] F. Lei, W. T. Crow, H. Shen, R. M. Parinussa, and T. R. H. Holmes, "The impact of local acquisition time on the accuracy of microwave surface soil moisture retrievals over the contiguous United States," *Remote Sens.*, vol. 7, no. 10, pp. 13448–13465, 2015.
[14] J.-P. Wigneron *et al.*, "L-band Microwave Emission of the Biosphere (L-MEB) model: Description and calibration against experimental data sets over crop fields," *Remote Sens. Environ.*, vol. 107, no. 4, pp. 639–655, Apr. 2007.
[15] Y. H. Kerr and E. G. Njoku, "A semiempirical model for interpreting microwave emission from semiarid land surfaces as seen from space," *IEEE Trans. Geosci. Remote Sens.*, vol. 28, no. 3, pp. 384–393, May 1990.
[16] T. Mo, B. J. Choudhury, T. J. Schmugge, J. R. Wang, and T. J. Jackson, "A model for microwave emission from vegetation-covered fields," *J. Geophys. Res., Oceans*, vol. 87, no. C13, pp. 11229–11237, Dec. 1982.
[17] M. C. Dobson, F. T. Ulaby, M. T. Hallikainen, and M. A. El-Rayes, "Microwave dielectric behavior of wet soil—Part II: Dielectric mixing models," *IEEE Trans. Geosci. Remote Sens.*, vol. GRS-23, no. 1, pp. 35–46, Jan. 1985.
[18] V. L. Mironov, M. C. Dobson, V. H. Kaupp, S. A. Komarov, and V. N. Kleshchenko, "Generalized refractive mixing dielectric model for moist soils," *IEEE Trans. Geosci. Remote Sens.*, vol. 42, no. 4, pp. 773–785, Apr. 2004.
[19] T. J. Jackson and T. J. Schmugge, "Vegetation effects on the microwave emission of soils," *Remote Sens. Environ.*, vol. 36, no. 3, pp. 203–212, 1991.
[20] O. Merlin *et al.*, "The NAFE'06 data set: Towards soil moisture retrieval at intermediate resolution," *Adv. Water Resour.*, vol. 31, no. 11, pp. 1444–1455, 2008.
[21] R. Panciera *et al.*, "The NAFE'05/CoSMOS data set: Toward SMOS soil moisture retrieval, downscaling, and assimilation," *IEEE Trans. Geosci. Remote Sens.*, vol. 46, no. 3, pp. 736–745, Mar. 2008.
[22] A. B. Smith *et al.*, "The Murrumbidgee soil moisture monitoring network data set," *Water Resour. Res.*, vol. 48, pp. 1–6, Jul. 2012.
[23] R. Panciera, M. Allahmoradi, O. Merlin, R. Young, and J. P. Walker, "The Hydraprobe Data Acquisition System (HDAS) V.5: User guide," Dept. Civil Eng., Univ. Melbourne, Melbourne, VIC, Australia, Tech. Rep., Nov. 2009.
[24] Y. H. Kerr *et al.*, "The SMOS soil moisture retrieval algorithm," *IEEE Trans. Geosci. Remote Sens.*, vol. 50, no. 5, pp. 1384–1403, May 2012.
[25] K. Saleh *et al.*, "The CoSMOS L-band experiment in Southeast Australia," in *Proc. IEEE Int. Geosci. Remote Sens. Symp. (IGARSS)*, Barcelona, Spain, Jul. 2007, pp. 3948–3951.
[26] J. P. Wigneron *et al.*, "Characterizing the dependence of vegetation model parameters on crop structure, incidence angle, and polarization at L-band," *IEEE Trans. Geosci. Remote Sens.*, vol. 42, no. 2, pp. 416–425, Feb. 2004.
[27] S. Peischl *et al.*, "The AACES field experiments: SMOS calibration and validation across the Murrumbidgee River catchment," *Hydrol. Earth Syst. Sci.*, vol. 16, pp. 1697–1708, Jun. 2012.
[28] J.-P. Wigneron, J.-C. Calvet, T. Pellarin, A. A. Van de Griend, M. Berger, and P. Ferrazzoli, "Retrieving near-surface soil moisture from microwave radiometric observations: Current status and future plans," *Remote Sens. Environ.*, vol. 85, no. 4, pp. 489–506, 2003.

Sandy Peischl (M'10) received the M.S. degree in geoecology from the Technische Universität Bergakademie Freiberg, Freiberg, Germany, in 2007, and the Ph.D. degree in environmental engineering from the Department of Civil Engineering, Faculty of Engineering, Monash University, Melbourne, VIC, Australia, in 2017.

Her research interests include the retrieval of soil moisture using multiincidence-angle L-band data acquired from airborne observations as well as from Soil Moisture and Ocean Salinity.

Jeffrey P. Walker (SM'12) received the B.E. degree (with Hons. 1 and University Medal) in civil engineering and the B. Surveying degree (with Hons. 1 and University Medal) in 1995 and the Ph.D. degree in water resources engineering from the University of Newcastle, Newcastle, NSW, Australia, in 1999. His Ph.D. dissertation was among the early pioneering research on estimation of root-zone soil moisture from remotely sensed surface soil moisture observations.

Since 2010, he has been a Professor with the Department of Civil Engineering, Faculty of Engineering, Monash University, Melbourne, VIC, Australia. He is contributing to soil moisture satellite missions at both NASA, Greenbelt, MD, USA, and the European Space Agency, Paris, France, as a Science Definition Team Member of the Soil Moisture Active Passive mission and a Calibration/Validation Team Member of the Soil Moisture and Ocean Salinity mission, respectively.

Dongryeol Ryu (M'05) received the B.S. and M.S. degrees in geology from Seoul National University, Seoul, South Korea, in 1997 and 2000, respectively, and the Ph.D. degree in earth system science from the University of California, Irvine, CA, USA, in 2006.

He is currently a Senior Lecturer with the Department of Infrastructure Engineering, Melbourne School of Engineering, University of Melbourne, Melbourne, VIC, Australia. His research interests include hydrology with particular emphases on remote sensing of land surface variables such as soil moisture and vegetation characteristics, their spatial and temporal variability, and hydrologic application of the remotely sensed land surface properties.

Yann H. Kerr (M'88–SM'01) received the B.E. degree from the Ecole Nationale Supérieure de l'Aéronautique et de l'Espace, Toulouse, France, the M.Sc. degree in electronics and electrical engineering from Glasgow University, Glasgow, U.K., and the Ph.D. degree from Université Paul Sabatier, Toulouse.

From 1980 to 1985, he was with the Centre National d'Etudes Spatiales (CNES), Toulouse. In 1985, he joined the Laboratoire d'Etudes et de Recherches en Télédétection Spatiale, Toulouse, where he was the Director from 1993 to 1994. From 1987 to 1988, for 19 months, he was with the Jet Propulsion Laboratory, Pasadena, CA, USA. Since 1995, he has been with the Centre d'Etudes Spatiales de la Biosphère, Toulouse, where he was the Deputy Director and has been the Director since 2007. In 1989, he was involved in the interferometric concept applied to passive microwave earth observation and was subsequently the Science Lead on the MIRAS project for the European Space Agency (ESA) with Maritime Management System and Operations Management Plan. In 1997, he first proposed the natural outcome of the previous MIRAS work with what was to become the Soil Moisture and Ocean Salinity (SMOS) mission to CNES, a proposal which was selected by ESA in 1999 with him as the Lead Investigator of the SMOS mission and the Chair of the Science Advisory Group. He is also in charge of the SMOS science activity coordination in France. His research interests include the exploitation of SMOS data, calibration/validation activities, related level-2 soil moisture and level-3 and level-4 development, and the SMOS next concept.